Sensors and Materials, Vol. 29, No. 7 (2017) 969–976
MYU Tokyo

S & M 1387

Nonvolatile Total Ionization Dose Radiation Sensor Using Titanium Nitride–Aluminum Oxide–Silicon Nitride–Silicon Oxide–Silicon Devices for High Response and Good Data Retention

Wen-Ching Hsieh,* Fuh-Cheng Jong,[1] Hao-Tien Daniel Lee,[2] and Shich-Chuan Wu[3]

Department of Opto-Electronic System Engineering, Minghsin University of Science and Technology,
Xinxing Road 1, Xinfeng 30401, Taiwan
[1]Electronic Engineering Department, Southern Taiwan University of Science and Technology,
1, Nan-Tai Street, Yungkang District, Tainan 710, Taiwan
[2]Treasure Giant Technology Inc., 3F-1, 42, Lyushuei Road, Hsinchu City 30068, Taiwan
[3]National Nano Device Laboratories, No. 26, Prosperity Road 1, Hsinchu Science Park, Hsinchu 30078, Taiwan

(Received April 8, 2016; accepted May 10, 2017)

Keywords: high-*k*, sensor, SONOS, MOS, radiation

The titanium nitride–aluminum oxide–silicon nitride–silicon oxide–silicon devices with a high-*k* aluminum oxide as a charge-blocking layer (TANOS) could be candidates for nonvolatile total ionization dose (TID) radiation sensors. Gamma radiation induces a significant decrease in the threshold voltage V_T of TANOS and the radiation-induced V_T decrease of TANOS is nearly 1.5 times that on a standard titanium nitride–silicon oxide–silicon nitride–silicon oxide–silicon (TONOS) device after 10 Mrad TID gamma irradiation. The change in V_T of TANOS after gamma irradiation also has a strong correlation to the TID up to 10 Mrad gamma irradiation. The V_T retention characteristics of TANOS devices can be improved before gamma irradiation and after 10 Mrad gamma irradiation. Moreover, the V_T retention characteristics of TANOS devices can be markedly improved and are nearly 10% better than those of standard TONOS devices after 10 Mrad gamma irradiation. Therefore, the TANOS device in this study has demonstrated the possibility of its use for high response and good TID data retention for nonvolatile TID radiation sensing.

1. Introduction

In various ionizing radiation applications such as space radiation monitoring and advanced semiconductor manufacturing processes with X-ray lithography, the measurement of total ionizing dose (TID) is a major concern. The commonly used dosimeters are ionization chambers and thermoluminescent dosimeters (TLDs). Semiconductor dosimeters offer many advantages over these traditional dosimeters, and their sensitivity can be very high in a small constrained space. A silicon–silicon dioxide–silicon nitride–silicon dioxide–silicon (SONOS) device has been shown to be suitable for nonvolatile, high TID radiation sensor applications.(1–10) The ionizing radiation induces a significant shift in the threshold voltage V_T of the SONOS device, and the V_T shift

---

[*] Corresponding author: e-mail: wchsieh@must.edu.tw

http://dx.doi.org/10.18494/SAM.2017.1600

has a strong correlation to TID up to 10 Mrad gamma irradiation. Moreover, the V_T retention characteristics of this nonvolatile SONOS device were good even after 10 years of retention.(1–10) However, a SONOS-type flash device with a high-*k* aluminum oxide (Al_2O_3) dielectric as the blocking layer has been found to provided faster W/E speed , lower gate leakage current, and longer data retention time.(11–13) The comparison of electrical performance between the titanium nitride–aluminum oxide–silicon nitride–silicon oxide–silicon (TANOS) and titanium nitride–silicon oxide–silicon nitride–silicon oxide–silicon (TONOS) devices after gamma irradiation, including radiation-induced charge density, gate leakage current, and charge retention reliability, were the main subjects of this study. From our experimental data, the radiation–induced charging effect and charge-retention reliability of a TANOS device was significantly better than that of a TONOS device. Therefore, a TANOS device was proposed to be more suitable for nonvolatile, high-TID radiation sensor applications.

2. Experimental Details

Six kinds of TONO devices prepared with different blocking layers for this experiment were compared, as indicated in Table 1: (1) TONOS using 100 Å SiO_2 as blocking layers (TO1NOS), (2) TANOS using 100 Å Al_2O_3 as blocking layers (TA1NOS), (3) TONOS using 200 Å SiO_2 as blocking layers (TO2NOS), (4) TANOS using 200 Å Al_2O_3 as blocking layers (hereafter TA2NOS), (5) TONOS using 300 Å SiO_2 as blocking layers (TO3NOS), and (6) TANOS using 300 Å Al_2O_3 as blocking layers (TA3NOS). All six TONOS devices in Table 1 were fabricated on p-type Si substrates. The thermal silicon oxide (SiO_2) was formed on the wafers as the tunneling oxide of all six TONOS devices (indicated in Table 1)using an ASM A-400 advanced clustered vertical furnace. After the tunneling oxide was formed, silicon nitride (nitride) (Si_3N_4) was deposited as the charge-trapping layer on the six TONOS devices by SVCS low-pressure chemical vapor deposition (LPCVD). The blocking SiO_2 was deposited by LPCVD using tetraethyloxysilane (TEOS) $[Si(OC_2H_5)_4]$ for the TONOS devices, and the blocking Al_2O_3 was formed by AIXTRON Tricent 800016 metal-organic chemical vapor deposition (MOCVD) at 450–550 °C for the TANOS devices. The control gate was formed of TiN metal using a ULVAC SBH-3308RDE DC sputtering machine. After gate patterning, the source and drain were formed by implantation of arsenic atoms and then activated at 900 °C for 30 s. For comparison, all devices listed in Table 1 had the same thicknesses of the tunneling oxide (30–70 Å SiO_2), trapping nitride (200–300 Å Si_3N_4), and metal gate (2000–4000 Å TiN). Figures 1(a) and 1(b) show the cross-sectional views of TONOS and TANOS devices, respectively.

For gamma TID data writing, ^{60}Co gamma radiation was irradiated onto all six TONOS devices at a negative gate bias stress (NVS) ($V_G = -4$ V). For the gamma TID data read, V_T was measured at room temperature using an Agilent HP4156A parameter analyzer. The experimental results

Table 1
Six kinds of TONOS devices.

Split	TO1NOS	TA1NOS	TO2NOS	TO2NOS	TO3NOS	TA3NOS
Charge-blocking layer	SiO_2	Al_2O_3	SiO_2	Al_2O_3	SiO_2	Al_2O_3
Blocking layer thickness	100 Å	100 Å	200 Å	200 Å	300 Å	300 Å

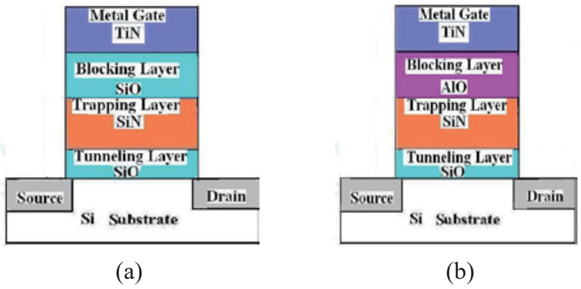

Fig. 1. (Color online) Cross-sectional views of (a) TONOS device and (b) TANOS device.

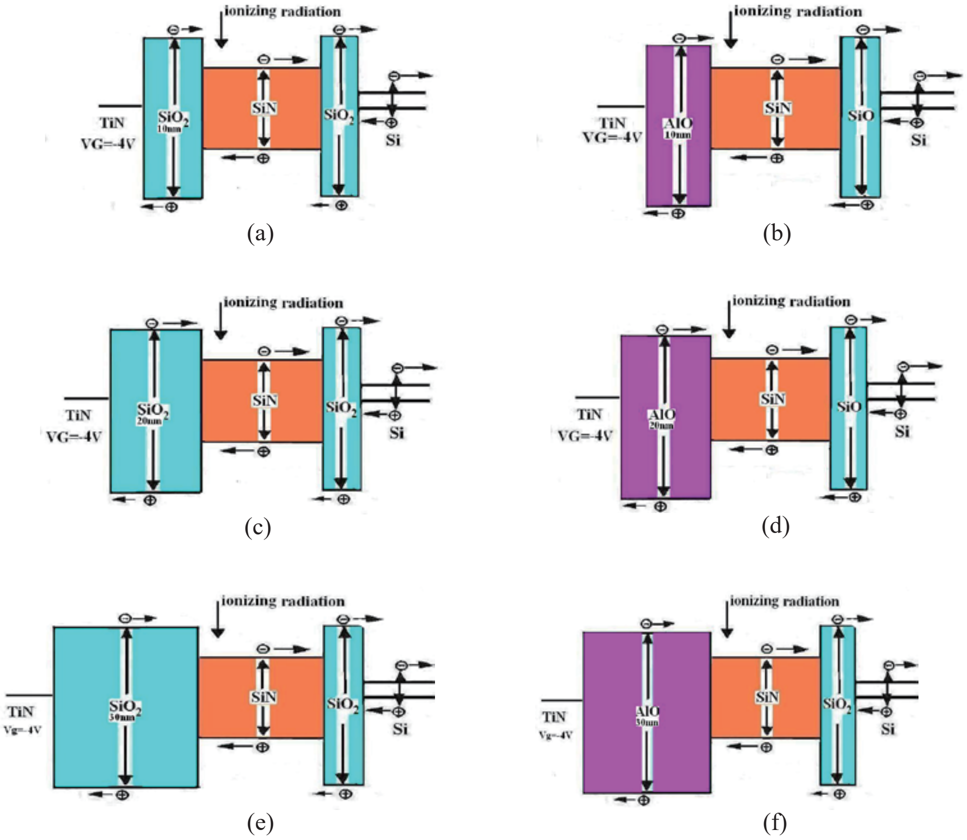

Fig. 2. (Color online) Radiation-induced charge generation and trapping in six kinds of devices: (a) TO1NOS, (b) TA1NOS, (c) TO2NOS, (d) TA2NOS, (e) TO3NOS, and (f) TA3NOS.

of gate leakage current under various gate voltages (I_G−V_G) were obtained using a computer-controlled Agilent HP4156 parameter analyzer. Figure 2 shows the radiation induced charges generated and trapped in the six kinds of TONOS devices indicated in Table 1. In Figs. 3(a) and 3(b), the wafer layouts for a TANOS capacitor and TANOS MOS are shown.

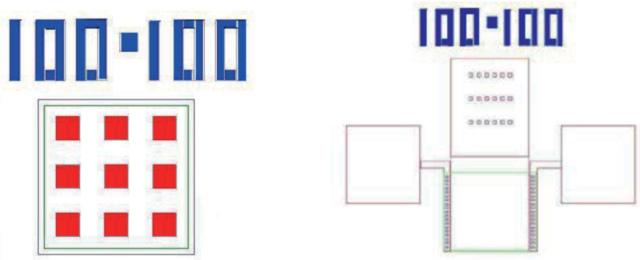

(a) (b)

Fig. 3. (Color online) The wafer layouts of (a) TANOS capacitor and (b) TANOS MOS.

3. Results and Discussion

3.1 Radiation-induced V_T shift in TANOS after gamma irradiation

Figure 4(a) shows the shift of the I_D–V_G curve for a TA3NOS device with NVS ($V_G = -4$ V) after 10 Mrad TID gamma irradiation. The I_D–V_G curve of TA3NOS shifted far to the left after 10 Mrad TID gamma irradiation. This indicates that gamma irradiation induces a large negative V_T shift in TA3NOS. The change is due to an large increase in net positive trapped charges in the aluminum oxide–silicon nitride–silicon oxide (ANO) gate dielectric layer after gamma irradiation. This negative V_T shift is in agreement with previous studies.(1–10) These radiation-induced negative V_T shifts in the irradiated TA3NOS device result from two effects. The first effect results from the loss of stored negative charge in the TA3NOS trapping layer after radiation. The second effect is due to a build up of positive charge resulting from asymmetric trapping of electrons and holes in the TA3NOS trapping layer after radiation.(1–10)

In Fig. 4(b), the decay of V_T for the TA3NOS device is plotted against the TID of gamma irradiation. The decrease in V_T of TA3NOS can be correlated to the increase in gamma TID. The decay of V_T increased more sharply after gamma irradiation levels up to 100 krad TID. The experimental results in this study are in agreement with previous studies.(1–10)

The radiation-induced V_T change and the relative radiation-induced charge density comparisons after 10 Mrad TID gamma irradiation for the six TONOS devices listed in Table 1 are illustrated in Figs. 5(a) and 5(b). The 10 Mrad radiation-induced V_T shift of TA3NOS is more significant than that of TO3NOS, as shown in Fig. 5(a), which results from more radiation-induced charges in the 300-Å-thick high-*k* Al_2O_3 blocking layer than in the 300-Å-thick traditional SiO_2 blocking layer. Similarly, the TA2NOS and TA1NOS devices with 200 Å and 100 Å Al_2O_3 blocking layers all demonstrate higher degrees of V_T shift than the TO2NOS and TO1NOS devices with 200 Å and 100 Å SiO_2 blocking layers. The radiation-induced charge density in ANO of the TA3NOS device with the thick Al_2O_3 blocking layer increased and was nearly 1.7 times that of the TO1NOS device with the thin SiO_2 blocking layer as illustrated in Fig. 5(b). However, the radiation-induced charge density in ONO of the TO3NOS device with the thick SiO_2 blocking layer decreased and was nearly 0.8 times that of the traditional TO1NOS device with the thin SiO_2 blocking layer. The trapped charge density was calculated by the Terman method.(14)

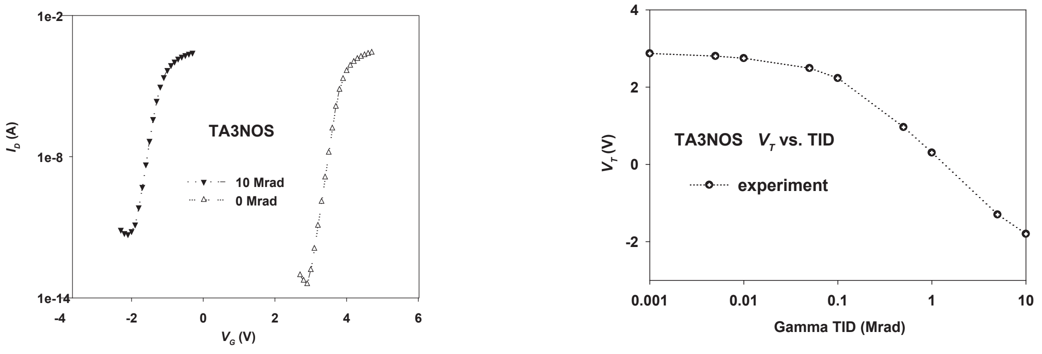

(a) (b)

Fig. 4. (a) Shift of the I_D–V_G curve after 10 Mrad gamma irradiation for TA3NOS device. (b) Dependence of V_T decrease on gamma TID for TA3NOS device.

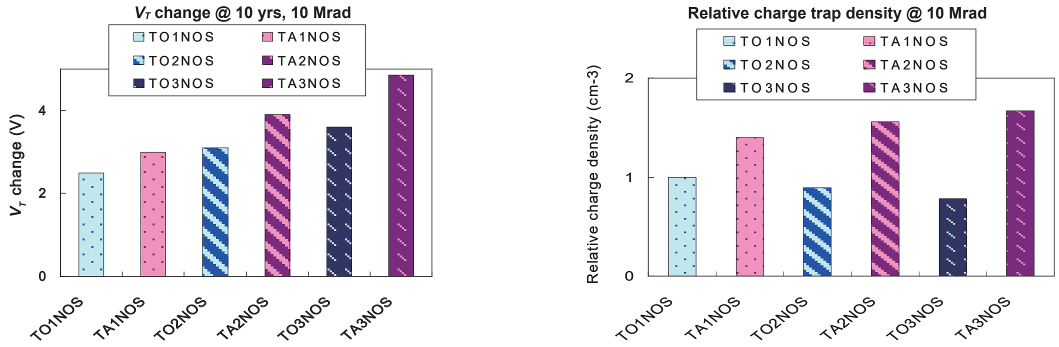

(a) (b)

Fig. 5. (Color online) (a) V_T changes induced by 10 Mrad gamma irradiation for six TONOS devices. (b) Relative charge density induced by 10 Mrad gamma irradiation for six TONOS devices.

3.2 Measurement of gate leakage current

The gate leakage current vs gate voltage (I_G–V_G) curves before irradiation and after 10 Mrad TID irradiation were plotted. As illustrated in Figs. 6(a) and 6(b), the gate leakage current of TA3NOS devices did not increase significantly after 10 Mrad TID gamma irradiation. Therefore, gate leakage current is assumed to not be the main factor contributing to the V_T shift of the TA3NOS device after 10 Mrad gamma irradiation. The experimental results in this study are in agreement with those of previous studies.(1–10)

Figures 7(a) and 7(b) show the gate leakage current under NVS ($V_G = -4$ V) for the six TONOS devices listed in Table 1 before gamma irradiation and after 10 Mrad TID gamma irradiation, respectively. The gate leakage current performance of TA3NOS is markedly improved over that of TO1NOS before gamma irradiation and after 10 Mrad TID gamma irradiation. However, the gate leakage current performance of TO3NOS is not obviously improved before gamma irradiation and after 10 Mrad TID gamma irradiation compared with that of TO1NOS. The experimental results in this study are in agreement with those of previous studies.(11–13)

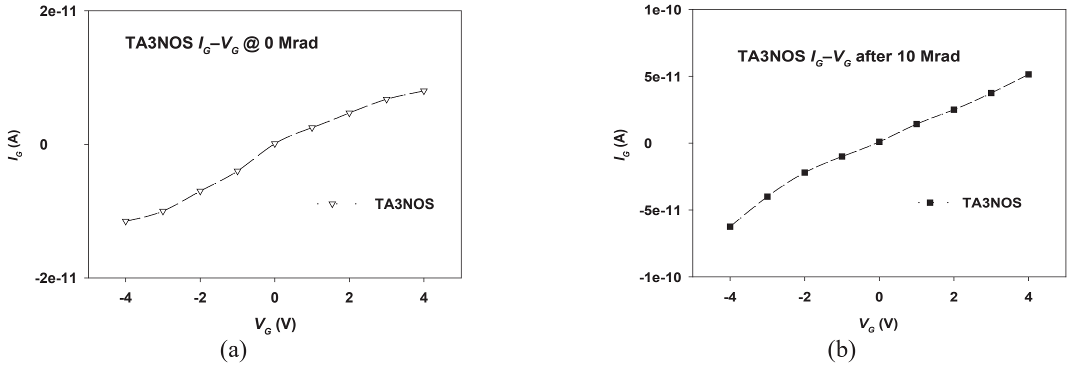

(a) (b)

Fig. 6. I_G–V_G curve for TA3NOS device (a) before gamma irradiation and (b) after 10 Mrad gamma irradiation.

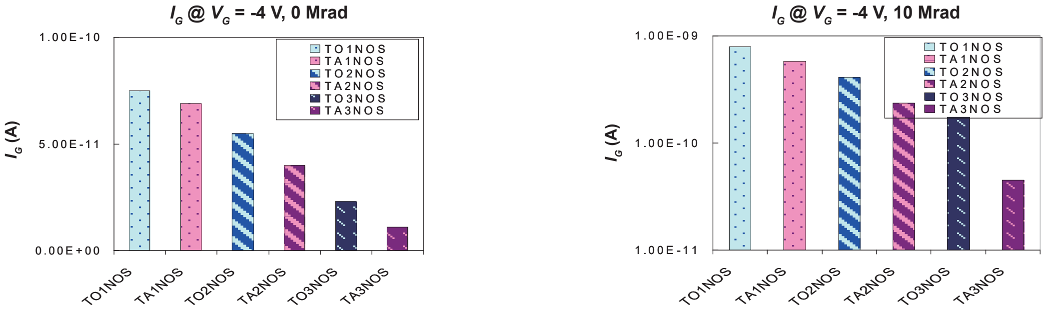

(a) (b)

Fig. 7. (Color online) gate-current under $V_G = -4$ V for six TONOS devices (a) before gamma irradiation and (b) after 10 Mrad gamma irradiation.

3.3 V_T stability vs retention time

Figures 8(a) and 8(b) show the V_T decay vs time (hereafter V_T–T) curve for an TA3NOS device under $V_G = -4$ V before gamma irradiation and after 10 Mrad gamma irradiation. The decrease in V_T with time for the pre-irradiated TA3NOS device under $V_G = -4$ V is a result of stored negative charges tunneling out of trapping nitride to the tunneling oxide, but the increase of V_T with time for the postirradiated TA3NOS device under $V_G = -4$ V is a result of radiation-induced positive charges tunneling out of the trapping nitride to the blocking layer. The experimental results in this study are in agreement with those of previous studies.(1–10) The predicted change in V_T after 10 years of retention was extrapolated from the experimental V_T–T curve obtained after 1 year of retention, as shown in Figs. 8(a) and 8(b).(1–10)

Figures 9(a) and 9(b) show the V_T change after 10 years of retention for six TONOS devices under $V_G = -4$ V before gamma irradiation and after 10 Mrad gamma irradiation. All the V_T changes for 10 years of retention were extrapolated from the experimental V_T–T curve obtained after 1 year of retention for the six TONOS devices.(1–10) The TANOS device with the high-*k* Al_2O_3 blocking layer showed better charge-retention reliability characteristics both before and after gamma irradiation than the traditional TONOS devices. The experimental results in this study are

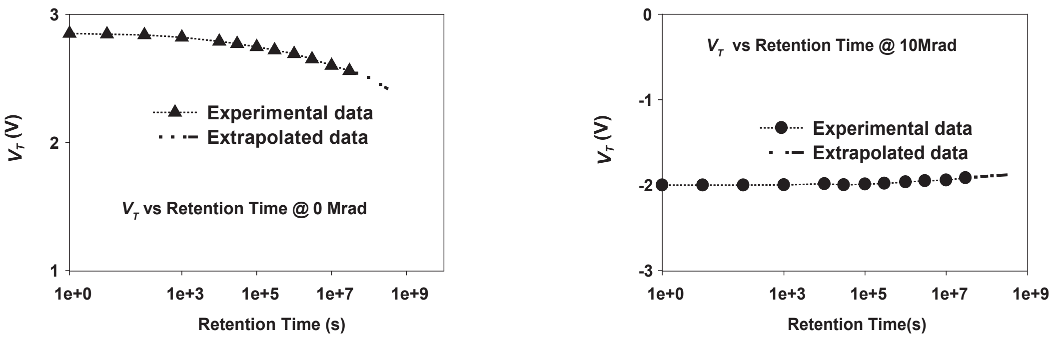

(a) (b)

Fig. 8. V_T decay vs time for TA3NOS device under $V_G = -4$ V (a) before gamma irradiation and (b) after 10 Mrad gamma irradiation.

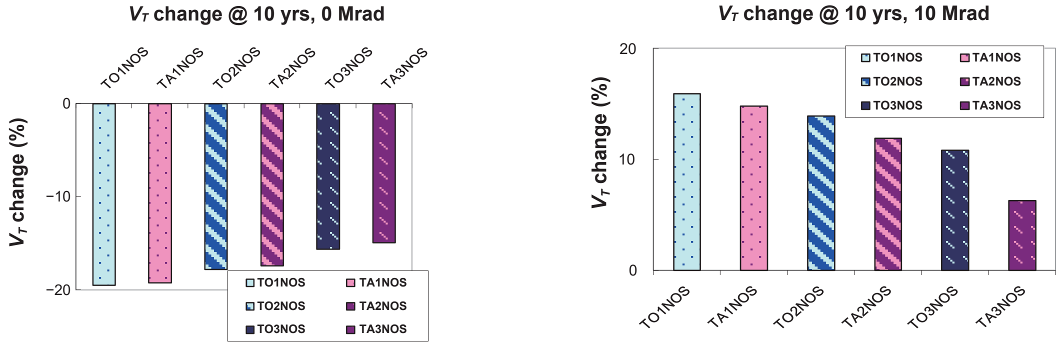

(a) (b)

Fig. 9. (Color online) V_T change after 10 years of retention for the six TONOS devices under $V_G = -4$ V (a) before gamma irradiation and (b) after 10 Mrad gamma irradiation.

in agreement with those of previous studies.(11–13) TA3NOS demonstrated marked improvement of the charge-retention reliability characteristics after 10 Mrad gamma irradiation compared with TA1NOS, TA2NOS, and TO3NOS devices, as shown in Fig. 9(b). However, the charge-retention reliability characteristics of TO3NOS are not appreciably improved beyond those of TO2NOS and TO1NOS devices. This result indicates that the thick high-*k* Al_2O_3 blocking layer of TA3NOS with large, deeper charge traps causes significant improvement in the charge-retention reliability characteristics compared with TO3NOS after 10 Mrad gamma irradiation under $V_G = -4$ V.

4. Conclusions

As shown in the experimental data, the radiation-induced charging effect of the TA3NOS device with high radiation-induced positive charge in the thick, high-*k* Al_2O_3 blocking layer is nearly 2 times that of the TO1NOS device with a thin traditional SiO_2 blocking layer after 10 Mrad gamma irradiation. The improvement in the radiation-induced charge retention reliability characteristics of the TA3NOS device with large, deeper charge traps in the thick Al_2O_3 blocking is nearly 10% better than that of the TO1NOS device with thin blocking SiO_2 after 10 Mrad gamma irradiation. However, the radiation-induced charge density and charge retention characteristics of the TO3NOS device with a thick SiO_2 blocking layer do not increase significantly compared with those of the TO1NOS device with a thin SiO_2 blocking layer after 10 Mrad gamma irradiation. The results obtained in this study demonstrated the feasibility of using a TA3NOS device for realizing high response and good TID information holding of nonvolatile radiation sensing up to 10 Mrad TID.

Acknowledgments

The authors thank the National Nano Device Laboratories (NDL), National Tsing Hua University (NTHU), and National Chiao Tung University (NCTU) for providing the instruments for wafer fabrication and testing. This study was funded in part by the National Science Council (NSC).

References

1 W. C. Hsieh, H. T. Lee, and F. C. Jong: Sensors **14** (2014) 14553.
2 W. C. Hsieh, H. T. Lee, F. C. Jong, and S. C. Wu: Sensors **4** (2016) 450.
3 W. C. Hsieh, H. T. Lee, F. C. Jong, and S. C. Wu: Sens. Mater. **5** (2016) 577.
4 W. C. Hsieh, H. T. Lee, F. C. Jong, and S. C. Wu: Sens. Mater. **9** (2016) 1023.
5 B. Draper, R. Dockerty, M. Shaneyfelt, S. Habermehl, and J. Murray: IEEE Trans. Nucl. Sci. **55** (2008) 3202.
6 F. Y. Qiao, X. Yu, and L. Y. Pan: Proc. 19th Int. Symp. Physical and Failure Analysis of Integrated Circuits (IPFA) (IEEE, 2012) p. 1.
7 F. Y. Qiao, L.Y. Pan, and J. Xu: IEEE Trans. Nucl. Sci. **61** (2014) 950.
8 S. Bassi and M. Pattanaik: Proc. 18th IEEE Int. Symp. VLSI Design and Test (VDAT) (IEEE, 2014) p. 1.
9 Y. Takahashi, K. Ohnishi, T. Fujimaki, and M. Yoshikawa: IEEE Trans. Nucl. Sci. **46** (1999) 1578.
10 T. R. Oldham and F. B. McLean: IEEE Trans. Nucl. Sci. **50** (2003) 483.
11 Y. N. Tan, W. K. Chim, W. K. Choi, M. S. Joo, and B. J. Cho: IEEE Trans. Electron Devices **53** (2006) 654.
12 S. Maikap, P. J. Tzeng, L. S. Lee, H. Y. Lee, C. C. Wang, P. H. Tsai, K. S. Chang-Liao, W. J. Chen, K. C. Liu, P. R. Jeng, and M. J. Tsai: 2006 Int. Conf. VLSI (IEEE, 2006) p. 1.
13 S. Choi, M. Cho, H. Hwang, and J. W. Kim: J. Appl. Phys. **94** (2003) 5409.
14 Y. Cheng, M. Ding, X. Wu, X. Liu, and K. Wu: 2013 Int. Conf. Solid Dielectrics (IEEE, 2013) p. 764.